

Deposition of Alumina-titania Nanostructured Coating by a New Multi-chamber Gas-dynamic Accelerator

M.G. Kovaleva², M.S. Prozorova², M.Yu. Arsenko², M.N. Yapryntsev², K.N. Mamunin², V.V. Sirota²,
A.Y. Altukhov¹, E.V. Ageev¹

¹ Southwest State University, 94, 50 Let Oktyabrya st., 305040, Kursk, Russia

² Belgorod National Research University, 85, Pobedy st., 308015 Belgorod, Russia

(Received 18 May 2016; published online 03 October 2016)

The aim of the study was to characterize alumina-titania ($\text{Al}_2\text{O}_3:\text{Ti}$ wt ratio = 87:13) coatings were deposited by a new multi-chamber gas-dynamic accelerator on a grit blasted steel substrate. The alumina-titania coatings were characterized using scanning electron microscopy, X-ray diffraction techniques and Vickers hardness tester at a test load 200 g. The coating was well-adhered onto corrosion-resistant steel substrate. Obtained coatings possessed a unique microstructure consisting of fully melted regions with the microstructure similar to a typical thermal sprayed lamellar morphology and areas comprising unmelted or partially melted particles. The dense alumina-titania coatings with hardness of $657 \pm 70 \text{ HV}_{0.2}$ and porosity of less than 0.6% have been prepared by a new multi-chamber gas-dynamic accelerator.

Keywords: Alumina–titania coatings, Multi-chamber gas-dynamic accelerator, Microstructure, Hardness.

DOI: [10.21272/jnep.8\(3\).03018](https://doi.org/10.21272/jnep.8(3).03018)

PACS numbers: 68.37.Hk, 68.37.Yz, 62.20.Qp

1. INTRODUCTION

Alumina coatings are an abrasion resistance coating example widely used in the cutting tool industry. Al_2O_3 -coated tool steel was found to be 2.5 times more resistant than uncoated tool steels [1]. When TiO_2 is added to Al_2O_3 , the toughness of the coating improves without changing the hardness. As the melting temperature of TiO_2 is lower, the melting point of Al_2O_3 lowers because TiO_2 can easily be connected to Al_2O_3 grains [2]. This improves coating performance. Depending on the application, different TiO_2 weight percentages are added to pure Al_2O_3 such as 3, 13 and 40 % [3]. Process of $\text{Al}_2\text{O}_3\text{-TiO}_2$ coatings formation is usually performed by means of APS, PVD, CVD, HVOF, detonation spraying and other methods [4, 5]. When the ceramic powders (Al_2O_3 , TiO_2) are introduced in the plasma stream, they are immediately melted and accelerated to spray a coating [6-8]. Generally, because of the process nature, the structure of a sprayed coating is characterized by the lamellar structures with the existence of the microdefects (pores, splat boundaries, microcracks, and some unmelted particles) [9]. The aim of the present study was to determine the microstructure of alumina-titania ($\text{Al}_2\text{O}_3:\text{Ti}$ wt ratio = 87:13) coating formed by a new multi-chamber gas-dynamic accelerator on a steel substrate combined with phase analysis, porosity, and hardness measurements.

2. EXPERIMENTAL PROCEDURE

In the present study, a multi chamber, vertically mounted gas-dynamic accelerator (MCDS) [10] was employed to deposit of the alumina-13wt. % titania coating. Characteristic feature of MCDS is that the powder is accelerated by using the combustion products, which are formed in the MCDS chambers and are converged before entering the nozzle, where they interact with the two-phase gas-powder cloud [11]. The spray parameters employed for depositing of alumina–13 wt. % titania coating are listed in Table 1. Prior to

spraying, a plate with dimensions of $30 \times 30 \times 5$ (mm) of the corrosion-resistant steel (Table 2) were degreased and grit blasted with 25A F360 alumina grits.

The starting powders used in this study were alumina powder (cheap raw material) and commercially available titanium powder PTS-2 (POLEMA JSC, Russia). SEM micrographs and XRD diffraction patterns of alumina and titanium powders are shown in Fig. 1.

The composite powder was prepared by solid state mixing route ($\text{Al}_2\text{O}_3:\text{Ti}$ wt ratio = 87:13).

Morphology, particle size, and particle size distribution of the powders were characterized using scanning electron microscope (QUANTA 200 3D, FEI) (SEM). The particle diameter was measured using a laser particle size analyzer (Analysette 22 NanoTec, FRITTSCH).

Table 1 – Process parameters used for depositing alumina-13 wt. % titania coating

Parameter	Value
Spray distance [mm]	65
Powder feed rate [g/h]	800
Frequency [Hz]	8
Barrel length [mm]	500
Barrel diameter [mm]	16
Flow rate of fuel mixture components, [m ³ /h]	
Oxygen	0.99*/1.26**
Propane (30 %) + butane (70 %)	0.22*/0.28**
Air	0.48*/0.6**
*Cylindrical form combustion chamber.	
**Combustion chamber in the form of a disk	

The obtained specimens were transversally cut by spark erosion, mechanically polished and prepared by standard metallographic sample preparation sectioning, mounting and polishing methods. This involved grinding with abrasive SiC paper. The specimens were then polished using 6, 3 and 1-micron diamond polishes on a lubricated cloth.

To determine the microstructure and elemental composition of the powder and coatings scanning electronic microscope (SEM) Quanta 200 3D was performed.

Phase composition of the powder and coatings was determined by the X-ray phase analysis method (diffractometer Rigaku Ultima IV).

Porosity was determined by the metallographic method with elements of the qualitative and quantitative analysis of the geometry of the pores using an optical inverted Olympus GX51 microscope [12]. Ten arbitrarily selected micrographs for each experimental point were registered with an optic microscope (bright

field, magnified 500x) using the "SIAMS Photolab" program.

Micro-hardness test was performed by an automatic micro-hardness tester DM-8B (Affri) on a cross section of coatings with a load of 200 g and dwell period of 15 sec. Indentation was carried out on cross-sections of the samples of the coatings, the distance between the indents being 20 μm . On average, 10 tests were used as an indicator of the coating hardness.

The all obtained samples are characterized by almost the same microstructures and hardness. Arbitrary selected data are presented in the paper.

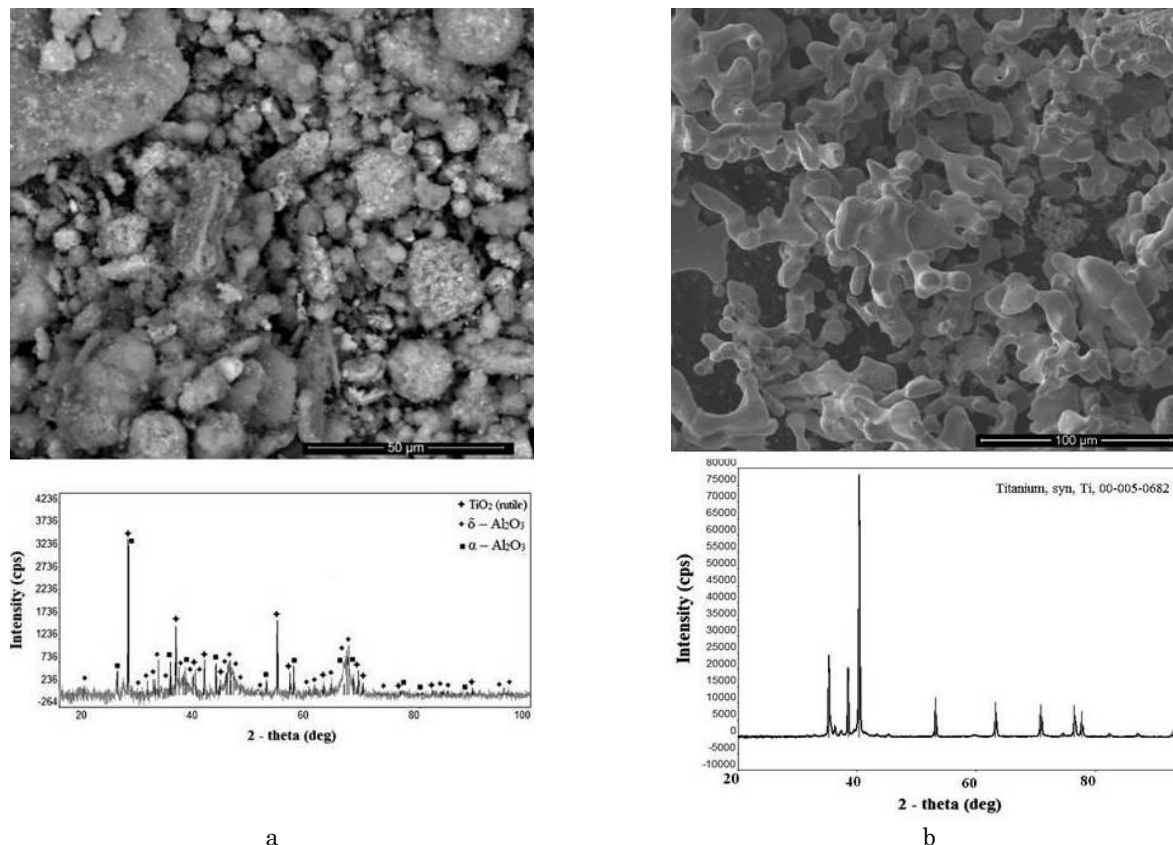


Fig. 1 – SEM micrographs and XRD diffraction patterns of powders (a) alumina and (b) titanium PTS-2 (back-scattered electron mode)

3. RESULTS AND DISCUSSION

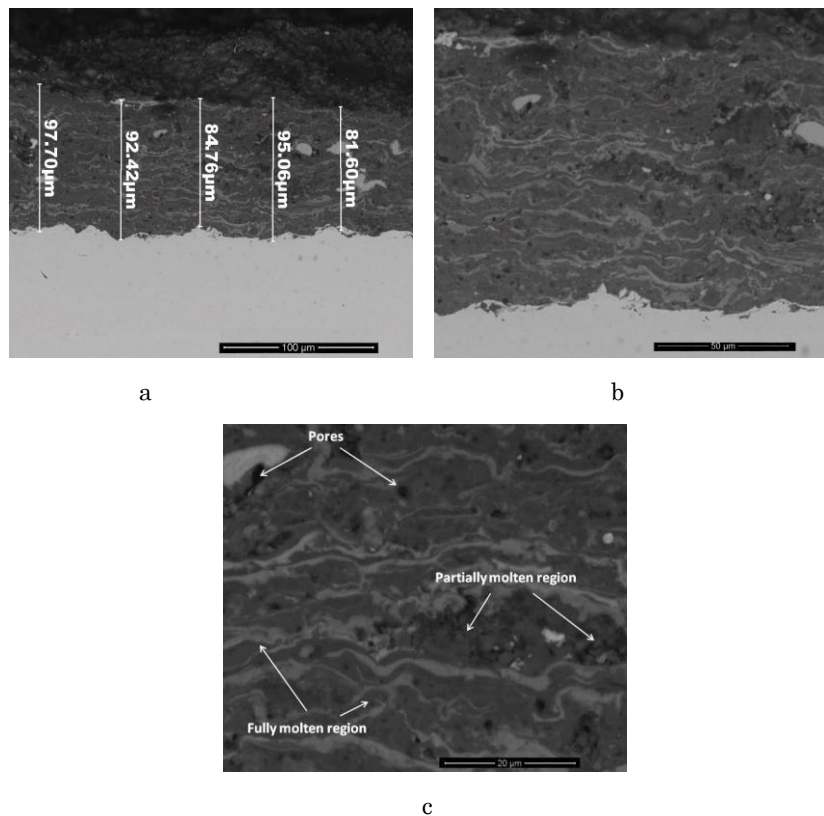
Fig. 2 presents scanning electron microscopy images taken at the backscattered electrons mode of the cross section of the alumina-13 wt. % titania coating. The thickness of observed coating was varied in the range of 80 to 100 microns, which resulted from the assumed investigated. The porosity of the alumina-13 wt. % titania coating was 0.57 ± 0.05 %. Measurement of porosity based on image analysis method agreed well with SEM micrographs. There are no visible macro defects between the coating and substrate. The coatings possessed a unique microstructure consisting of fully melted regions with the microstructure similar to typical thermal sprayed lamellar morphology and regions

comprising unmelted or partially melted particles. It was found that most powders were fully or partially melted during spraying (Fig. 2c).

The XRD pattern of obtained coatings is shown in Fig. 3. In the specimen coated by alumina-13 wt. % titania coatings, XRD data give Ti, TiO, TiO₂ (rutile) phases beside γ -Al₂O₃ and α -Al₂O₃ phases (Fig. 3, Table 2). The powder comprised of γ -Al₂O₃, α -Al₂O₃ and TiO₂ phases (Fig. 1, Table 2). During spraying process, a stable α -Al₂O₃ was transformed to a metastable γ -Al₂O₃. It had been suggested that the γ -phase always homogeneously nucleated in the rapid quenching of completely melted droplets because of its critical free energy for nucleation from the liquid was less than that of the α -phase [13].

Table 2 – The chemical composition, phase composition of powder and coatings, and microhardness of alumina-13 wt. % titania coatings

	Powder		Coating	Steel
	Alumina	Titanium		
Chemical composition, all in wt pct		Ti-86.40	Ti-28.47	Cr-17.5
	O-37.13	Fe-0.16	Al-31.63	Ni-9.4
	Al-48.94	Si-1.61	Fe-9.46	C-0.06
	Ca-0.58	Ca-0.39	Cr-2.39	Si-0.5
	Ti-9.87	C-5.85	O-21.93	Mn-1.2
	Fe-3.01	O-3.66	C-5.25	P-0.02
	Zr-0.47	Al-1.39	Ni-0.92	S-0.02
		Cr-0.28	Ti-0.48	
Particle size distribution [μm]				
d(0.1)	5.4	11.29		
d(0.5)	34.22	48.63		
d(0.9)	58.80	91.31		
Identified major phases	$\gamma\text{-Al}_2\text{O}_3$ $\alpha\text{-Al}_2\text{O}_3$ TiO_2 (rutile)	Ti	$\eta\text{-(Al}_{2.144}\text{O}_3)_{3.2}$ $\gamma\text{-(Al}_2\text{O}_3)_{1.333}$ $\alpha\text{-Al}_2\text{O}_3$ Ti TiO TiO_2 (rutile)	–
Porosity, [%]	–	–	0.57 \pm 0.05	–
Microhardness, [$\text{HV}_{0.2}$]	–	–	657 \pm 70	187 \pm 11

**Fig. 2** – SEM BSE microstructure of obtained alumina-13 wt. % titania coating

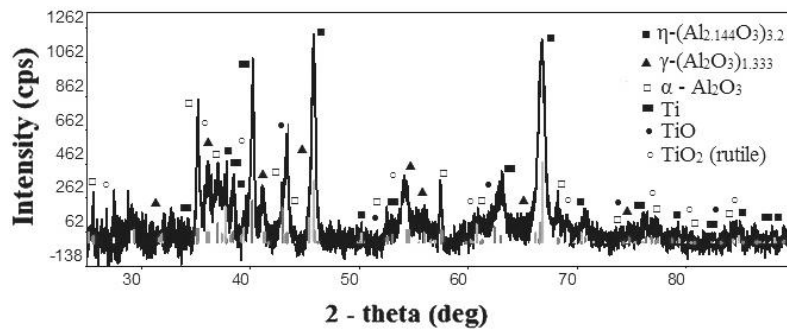


Fig. 3 – XRD pattern of the coating layer

The final hardness value of alumina-13 wt. % titania coating determined at level $657 \pm 70 \text{ HV}_{0.2}$ is an average of 10 measurements performed at different locations on the coating cross section. They are in agreement with the work by Geetha et al. [14] ($760 \pm 18 \text{ HV}_{0.2}$).

In comparison to the substrate, the microhardness of the alumina-13 wt. % titania coating produced using a new multi-chamber gas-dynamic accelerator was 3.5-4 times harder.

4. CONCLUSIONS

Corrosion-resistant steel substrate was coated with powder composition alumina-titania (87-13 wt %) by a new multi-chamber gas-dynamic accelerator in open

atmosphere. The microstructures and their formation mechanisms during spraying were discussed. Uniform and dense coating layers which are harder 3.5-4 times of the substrate were obtained. XRD results revealed that the coating contained Ti, TiO, TiO₂ (rutile) phases beside $\gamma\text{-Al}_2\text{O}_3$ and $\alpha\text{-Al}_2\text{O}_3$ phases.

ACKNOWLEDGEMENTS

The study was financial supported by the Russian Science Foundation, under grant No 15-19-00189. All of studies were carried out on the equipment of the Joint Research Center of Belgorod National Research University «Diagnostics of structure and properties of nanomaterials».

REFERENCES

1. J.H. Ouyang, S. Sasaki, K. Umeda, *Surf. Coat. Technol.* **137**, 21 (2001).
2. M. Harju, E. Levänen, T. Mäntylä, *Appl. Surf. Sci.* **252**, 8514 (2006).
3. J. Ilavsky, C.C. Berndt, H. Herman, P. Chraska, J. Dubsy, *J. Therm. Spray Technol.* **6**(4), 439 (1997).
4. S. Kumar, J.S. Ratol, *Mater. Eng.* **20**, 119 (2013).
5. V. Ulianitsky, V. Shtertser, I. Smurov, *J. Therm. Spray Technol.* **20**(4), 791 (2011).
6. T. Irisawa, H. Matsumoto, *Thin Solid Films* **509**, 141 (2006).
7. Z. Yin, S. Tao, X. Zhou, C. Ding, *J. Eur. Ceram. Soc.* **28**, 1143 (2008).
8. P. Ctibor, P. Bohac, M. Stranyanek, R. Ctvrtlik, *J. Eur. Ceram. Soc.* **26**, 3509 (2006).
9. P. Fauchais, A. Vardelle, A. Denoirjean, *Surf. Coat. Technol.* **97**, 66 (1997).
10. N. Vasilik, Yu. Tyurin, O. Kolisnichenko, RU Patent 2.506.341 (2012).
11. M. Kovaleva, Y. Tyurin, N. Vasilik, O. Kolisnichenko, M. Prozorova, M. Arseenko, E. Danshina, *Surf. Coat. Technol.* **232**, 719 (2013).
12. G.J. Moskal, *JAMME*, **20** (1-2), 483 (2007).
13. M.U. Devi, *Ceram. Int.* **30**(4) 555 (2004).
14. M. Geetha, S. Sathish, K. Chava, S.V. Joshi, *Surf. Eng.* **30**(4), 229 (2014).